Universality in axisymmetric vacuum collapse

Andrew M. Abrahams*
Center for Radiophysics and Space Research, Cornell University, Ithaca, New York 14853

Charles R. Evans
Department of Physics and Astronomy, University of North Carolina, Chapel Hill, North Carolina 27599
(Received 19 October 1993)

Evidence of universality is observed in the critical behavior of axisymmetric vacuum gravitational collapse. The threshold of black hole formation in the future development of time-antisymmetric initial data is found numerically and compared to previous results based on ingoing pulses of gravitational waves. The power-law behavior of the black hole mass is again found near the critical point and the critical exponent value $\beta \simeq 0.36$ is consistent with our previous determination despite stark differences in the two sets of initial data. Similar evidence of universality is exhibited by the scaling factor Δ of the echoes in the gravitational field produced in the central region of collapse.

PACS number(s): 04.20.Jb, 02.60.Cb, 04.30.Nk, 97.60.Lf

I. INTRODUCTION

Critical phenomena have recently been shown to occur near the threshold of black hole formation in several types of gravitational collapse. This behavior was first observed in the collapse of scalar waves in spherical symmetry [1] and subsequently in the collapse of gravitational waves in axisymmetry (Ref. [2], hereafter paper 1). Critical phenomena have now also been observed in radiation fluid collapse [3]. The vacuum case is significant because it implies these phenomena are generic features of general relativity.

A process for finding the threshold of black hole formation and associated critical phenomena is to compute the future development $\mathcal{S}_k[p]$ of elements of single-parameter families of Cauchy data, with p labeling the data sets within a family and k labeling different families. Solutions are computed numerically and the critical point $p^\star$ of onset of black hole formation in any family is narrowed down by bisection. In this way, $p^\star$ separates supercritical from subcritical solutions and one can view p as characterizing the strength of the ensuing gravitational self-interaction.

Not all parametrizations of Cauchy data will suffice. In the vacuum gravity case studied here and in paper 1, we know from the work of Christodoulou and Klainerman [4] that Cauchy data comprised of sufficiently weak gravitational waves avoid the future formation of singularities. In contrast, Beig and O'Murchadha [5] have given sufficient conditions that configurations of gravitational waves produce apparent horizons, and presumably black holes. As we showed in paper 1 and show here, the constructive process of locating the black hole threshold works in vacuum collapse because at least some parametrizations of the initial data can be found to smoothly interpolate between weak and strong field limits.

Critical behavior is observed as $p \to p^\star$. In near-critical solutions with $p > p^\star$, the black hole mass is found to have a power-law dependence on critical separation: $M_{\rm BH} \propto (p - p^\star)^\beta$. Choptuik [1] found the critical exponent in scalar field collapse to be near $\beta \simeq 0.37$ and universal in the sense of being independent of the details of the initial data. In paper 1, we investigated a sequence of initial data representing ingoing gravitational wave pulses. We also found that near the critical point the black hole mass follows a power law and that it has a critical exponent that is numerically indistinguishable from the scalar-field case. This power-law behavior implies that in classical general relativity processes exist whereby, in principle, infinitesimal black holes can be formed, possibly representing a violation of cosmic censorship [6]. The power-law behavior also allows an analogy to be drawn to static critical phenomena, suggesting a natural association of black hole mass with an order parameter [2].

Another connection with standard critical phenomena is the observation of self-similarity, or scaling [7], in near-critical solutions. In both scalar-field collapse and gravitational wave collapse, the nonlinearities induce the fields to oscillate in a scale-free, self-similar fashion that becomes evident in near critical solutions with $p \simeq p^\star$. For example, in the scalar field case [1] the scalar field ϕ asymptotically approaches a scaling relation (or discrete self-similarity) of the form

$$\phi(\rho - \Delta, \tau - \Delta) \simeq \phi(\rho, \tau), \tag{1}$$

where ρ and τ are logarithms of proper (areal) radius R and central proper time T: $\rho = \ln R + \kappa$ and $\tau = \ln(T^\star - T) + \kappa$. The time $T^\star$ can only be determined

*Also at the Laboratory of Nuclear Studies and Center for Theory and Simulation in Science and Engineering, Cornell University.

after the search locates $p^\star$ and it represents the finite accumulation time of the infinite number of echoes implied by Eq. (1). The constant κ is a family-specific length scale. Choptuik [1] found $\Delta \simeq 3.4$ and evidence that it too is universal. As reported in paper 1, we also observed oscillations in the vacuum gravitational field in the central region of collapse. Using oscillations of the central value of the lapse function to time the echoes, we found evidence of scaling in the radial dependence of the metric. For example, the metric variable η (defined below) was found to scale like

$$\eta(\rho - \Delta_\rho, t_n) \simeq \eta(\rho, t_{n+1}), \tag{2}$$

where $\rho = \ln r$ is the logarithm of the quasi-isotropic radial coordinate and t_n label the coordinate times of maxima in the central value of the lapse function. We distinguish between radial and temporal scaling constants, though $\Delta_\rho = \Delta_\tau$ is anticipated based upon results in scalar-field collapse [1]. In paper 1 we were only able to determine a radial scaling constant and found it to be $\Delta_\rho \simeq 0.59$, quite different from the scalar-field case. The value of Δ_τ, expressing the differences in the logarithm of central proper times associated with times t_n, could not be determined sufficiently well.

In this paper, we present results obtained from a new sequence of spacetimes generated by initial data that is starkly different from that considered in paper 1. The properties of near-critical spacetimes in this new sequence, when compared to those of paper 1, provide evidence of the universality of both β and Δ_ρ. These new calculations also allow us to probe closer to the critical point and to estimate the time-scaling constant Δ_τ. In Sec. II we briefly describe the gravitational field variables and give the form of the new Cauchy data. In Sec. III our numerical results are discussed and compared with our earlier calculations.

II. TIME-ANTISYMMETRIC CAUCHY DATA

We compute axisymmetric, asymptotically flat vacuum spacetimes using the 3+1 formalism [8], with the maximal time-slicing condition and quasi-isotropic spatial gauge. Details of the equations we solve can be found elsewhere [2,9]. Here we mention the gravitational field variables in order to describe the Cauchy data. The line element in these coordinates is

$$ds^2 = -\alpha^2 dt^2 + \phi^4[e^{2\eta/3}(dr + \beta^r dt)^2 + r^2 e^{2\eta/3}(d\theta + \beta^\theta dt)^2 + e^{-4\eta/3} r^2 \sin^2\theta d\varphi^2], \tag{3}$$

where α is the lapse function, β^r and β^θ are shift vector components, ϕ is the conformal factor, and η is an even-parity, "dynamical" metric function. The symmetries and the time-slicing condition reduce the number of linearly independent extrinsic curvature components to three, and for these we use the projection of $K^i{}_j$ on the spatial coordinate basis: $\lambda = K^r{}_r + 2K^\varphi{}_\varphi$, $K^\varphi{}_\varphi$, and $K^r{}_\theta$. The momentum constraints further restrict these, so that only one component is freely specifiable. Similarly, the conformal factor ϕ must satisfy the Hamiltonian constraint, making η the only freely specifiable part of the three-metric. The shift components β^r and β^θ and lapse function α are determined by the kinematical conditions.

Previously we investigated imploding pulses of gravitational waves and found critical phenomena [2,10]. Here we compute the future development of time-antisymmetric initial data (the same solution results if $K^i{}_j \to -K^i{}_j$ and $t \to -t$), which are constructed so as to concentrate mass energy in a compact region from the outset. Primarily because of its simpler structure and initial concentration, the time-antisymmetric initial data have enabled us to probe closer to the critical point. In order to be able to extend our parametrized Cauchy data to the weak-field limit and there have analytic expressions, we use the form of a general linear solution as a basis for construction all of the data sets. The general solution to the equations of linearized gravity [11] for a quadrupole $\ell = 2$ wave, when transformed to quasi-isotropic coordinates and maximal slices, gives the following time-antisymmetric form for η and $K^r{}_\theta$ after adding outgoing and ingoing parts:

$$\eta = \left(\frac{I^{(2)}(u) - I^{(2)}(v)}{r} + 2\frac{I^{(1)}(u) + I^{(1)}(v)}{r^2} + \frac{b_2(t)}{r^2}\right)\sin^2\theta, \tag{4}$$

$$\frac{K^r{}_\theta}{r} = \left(\frac{I^{(2)}(u) + I^{(2)}(v)}{r^2} + 3\frac{I^{(1)}(u) - I^{(1)}(v)}{r^3} + 6\frac{I(u) + I(v)}{r^4} + 6\frac{I^{(-1)}(u) - I^{(-1)}(v)}{r^5}\right)\sin 2\theta. \tag{5}$$

The solution involves derivatives of an arbitrary function $I^{(-2)}$ [where $dI^{(k)}(x)/dx = I^{(k+1)}$ and where I itself is the quadrupole moment] of retarded $u = t - r - r_0$ or advanced $v = t + r - r_0$ time, with r_0 an initial radius. We choose $r_0 = 0$ so the mass energy is concentrated near the origin. We set $b_2(t = 0) = -2I^{(1)}(0)$, which is necessary to ensure the regularity of the initial data at the origin. Equations (4) and (5) are taken as the forms of the freely specifiable data regardless of the proximity to the weak-field limit. To compute derivatives conveniently and to concentrate the mass-energy initially, the function $I^{(-2)}(x)$ is taken to have the form

$$I^{(-2)}(x) = ac_n\Lambda^5 H_n(x/\Lambda)e^{-x^2/\Lambda^2}, \qquad (6)$$

where a is an amplitude parameter, $c_n = \{(225/8\pi)^2/[(2n+1)!!]\}^{1/4}$ is a normalization constant, Λ is a width parameter, and H_n are Hermite polynomials. [Note that these functions $I^{(k)}(x)$ are not Hermite functions.] We consider only the $n = 0$ case. On substitution of (6) in (4) and (5), we find that $\eta = 0$ initially, while $K^r{}_\theta \neq 0$. The choice of sign of a is physically significant and we examined models with $a > 0$ only. Values of the parameter a which lead to near-critical future developments give initial data that are far from the weak-field limit. Consequently, specification of the initial data is completed by solving the momentum and Hamiltonian constraint equations to determine λ, $K^\varphi{}_\varphi$, and ϕ. The time-antisymmetric initial data are pictured in Fig. 1 and compared to the data for ingoing pulses that were used in our original study (paper 1).

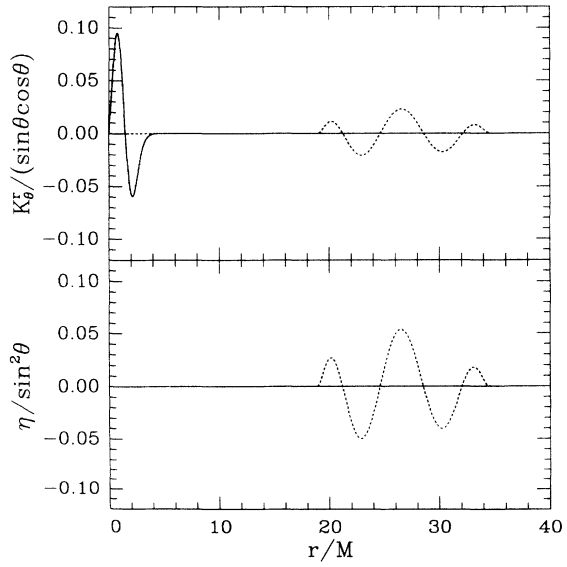

FIG. 1. Comparison of time-antisymmetric and ingoing-pulse gravitational wave initial data. The initial radial profiles of the freely specifiable parts of the gravitational field, η (lower frame) and $K^r{}_\theta$ (upper frame), are shown for near-critical parameter values. The two data sets have been scaled to a common mass or length scale. Time-antisymmetric fields are plotted as solid curves while the ingoing-pulse fields are shown as dotted curves.

III. EVIDENCE OF UNIVERSALITY

All of the results displayed in this paper were computed at a resolution of 340 radial and 26 angular zones (over one quadrant). A comparison was made with models computed with 380 by 38 zones, representing a factor of 1.5 decrease in discretization scale (the radial grid is geometrically spaced). A moving-mesh algorithm [9] was employed to maintain resolution of the collapsing, self-similar region and, for supercritical models, of the black holes which form. Gravitational waveforms are extracted at several radii between Λ and 4Λ and the outer boundary of the calculation is set to $r_{\rm out} \simeq 40M_p \simeq 17\Lambda$, where M_p is the initial total mass [2,12] which is used to parametrize all dimensional quantities. Our initial data sequence is generated by varying the amplitude parameter a. The critical value was found to be $a^\star \simeq 6.387\,495$. The number of significant figures given should be taken as an indication of the precision of our numerical bisection not of absolute accuracy. The actual value of $a^\star$ we determine is dependent on the details of our mesh and numerical scheme. For convenience, we have summarized in Table I the critical parameters determined for both the new time-antisymmetric initial data and the ingoing-pulse initial data.

In Fig. 2 we show the central value of the lapse function

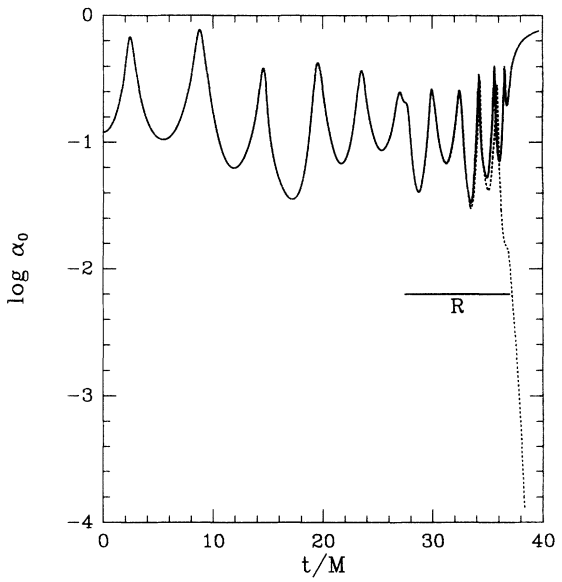

FIG. 2. Evolution of the central value of the lapse function for near-critical evolutions of time-antisymmetric Cauchy data. The logarithm (to the base 10) of the central value of the lapse is shown for supercritical (solid curve) and subcritical (dotted curve) models as a function of coordinate time in units of the packet mass M_p. The first 12 extrema, approximately, can be associated with the structure of the initial data. The subsequent oscillations reflect echoes generated by the nonlinear self-interaction. In the subcritical case the lapse approaches unity at late times as the mass energy disperses. In the supercritical case the lapse finally begins to vanish exponentially as a black hole forms. The period of echoing is indicated by the horizontal bar.

TABLE I. Parameters of initial data sequences with error estimates.

Initial data	$a^\star$	β	Δ_ρ	Δ_τ	Max. $M_{\rm BH}/M_p$	Min. $M_{\rm BH}/M_p$
Ingoing pulse	0.928 ± 0.002	0.37 ± 0.02	0.60 ± 0.05	...	0.95 ± 0.02	0.19 ± 0.02
Time antisymmetric	6.3875 ± 0.0001	0.36 ± 0.03	0.54 ± 0.05	0.51 ± 0.03	0.45 ± 0.01	0.058 ± 0.01

$\alpha_0 \equiv \alpha(r = 0, t)$ for two near-critical evolutions. Each of these cases has $|(a - a^\star)/a^\star| < 2 \times 10^{-6}$. Roughly, the first 12 extrema in the oscillations of $\alpha_0(t)$ appear to be primarily caused by the particular shape of the initial data. The subsequent oscillations are a manifestation of the echoing of the field seen in near-critical solutions. This determination has been made both experimentally by attempting to fit the early lapse oscillations to scaling laws, and by finding close correspondence between the structure of the initial data and that of the initial oscillations of the lapse.

As before, when a black hole forms, its mass is determined redundantly by calculating the area of the apparent horizon and by analyzing the $\ell = 4$ waveform and fitting it with a superposition of $\ell = 4$ quasinormal modes [2,9,10]. In Fig. 3, we plot mass as a function of critical separation for both the time-antisymmetric and ingoing pulse (paper 1) families. The smallest black hole we form in the new calculations has a mass $M_{\rm BH} = 0.05 M_p$. We find that for these time-antisymmetric configurations trapping more than about one-half of the original wave packet requires $a \gg a^\star$. This may depend strongly on the sign choice of $a > 0$ and reflect a strong divergence of radial null rays in the initial data. The upper frame of Fig. 3 shows that, close to the critical point, the black hole mass obeys a power law with an exponent $\beta \sim 0.36 - 0.37$ that is numerically consistent with that found in the ingoing-pulse sequence of paper 1. This coincidence of values of the critical exponent, despite stark differences in the initial data, suggests that the value of β is universal.

In Fig. 4 we show two radial profiles of the metric function η, one obtained from the ingoing-pulse sequence of paper 1 and the other obtained from the time-antisymmetric sequence. Both are from very near-critical evolutions. Each family of solutions can be renormalized by a change in the mass scale associated with the initial data. A change in the mass scale does not affect the amplitude of η but will alter the radial coordinate, or introduce a constant offset κ in $\rho = \ln r$. This single number is all the information about the initial data that the solution retains in the asymptotic region ($r \to 0$) and it reflects only a trivial change of scale. In Fig. 4, we rescale (shift by some κ) one profile to match the other at small radii. The apparent convergence and considerable agree-

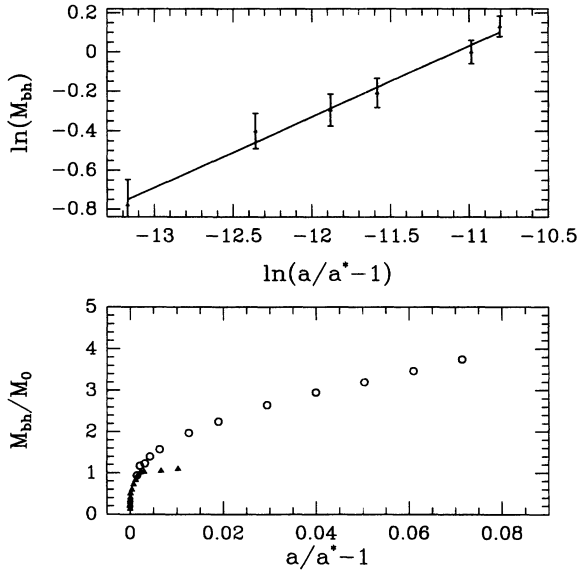

FIG. 3. Critical behavior of black hole mass. The bottom frame compares, on a linear scale, the black hole mass as a function of the critical separation $a - a^\star$ for the time-antisymmetric (solid triangles) and ingoing-pulse (open circles) sequences. The masses in the time-antisymmetric cases have been scaled by the factor $M_0 = 3.3$. The top frame shows, on a log-log scale, the best-fit power law for black hole mass obtained from six of the nearest-critical, time-antisymmetric evolutions. The slope of the fit yields a critical exponent value of $\beta = 0.36$.

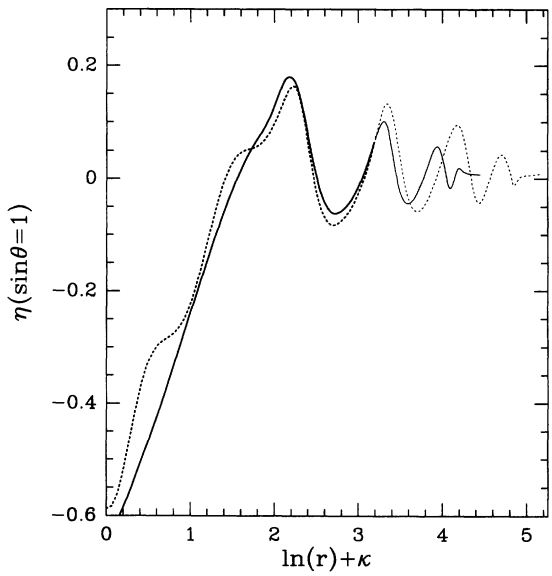

FIG. 4. Universality of the echoes in the gravitational field. Equatorial slices of the metric function η are compared for two very near critical, but subcritical, solutions. One of these (solid curve) is a time-antisymmetric model while the other (dotted curve) is an ingoing-pulse model. Bold parts of the curves highlight the self-similar portions of the oscillations. A rescaling of the mass scale, implying $\log r \to \log r + \kappa$, is chosen to demonstrate the agreement between the solutions at small radii.

ment between these separate computations of the echoes in the gravitational field lend support to the contention that there exists a unique, discretely self-similar solution which all precisely critical models approach in the central region of collapse and which very near critical solutions approach on intermediate length scales.

The time-antisymmetric data, by enabling us to compute models nearer the critical point, allow an estimate of the time-scaling constant Δ_τ to be made. The time of a given central lapse extremum labeled by N is given by

$$\tau_N \simeq \tau_0 + \sum_{n=1}^{N} \delta\tau_0 \exp[-\Delta_\tau(n-1)], \tag{7}$$

where τ_0 is the central proper time corresponding to the beginning of the strong-field oscillations and $\delta\tau_0$ is the duration of the first echo. Thus, the central proper-time duration of each echo obeys a power law of the form $d\tau/dN = K\exp(-\Delta_\tau N)$. Each near-critical echo corresponds to two central lapse oscillations or four extrema. In Fig. 5 we show data points and the results of a power-law fit for our deepest supercritical model, $a = 6.8375$. Data points are shown for each lapse extremum; each near-critical echo corresponds to two central lapse oscillations or four such extrema. We obtain a scaling constant in the range $\Delta_\tau = 0.49 - 0.54$.

The upper panel of Fig. 6 shows overlapped radial profiles of η from the same supercritical model. These were overlapped after obtaining a best-fit radial scaling constant of $\Delta_\rho = 0.50$, which is in agreement with the fit for Δ_τ. The second panel shows the radial profiles from a subcritical model. From these data, we obtain an estimated radial scaling constant of $\Delta_\rho \sim 0.58$, which is consistent with that obtained in paper 1 from ingoing-pulse models. We ascribe no significance to this difference but rather view it as a measure of the uncertainty in the determination of Δ_ρ. We believe it reflects the present limitation in computing in closer proximity of the critical point and an associated limitation on the range of length scales between which the solution approaches self-similar form.

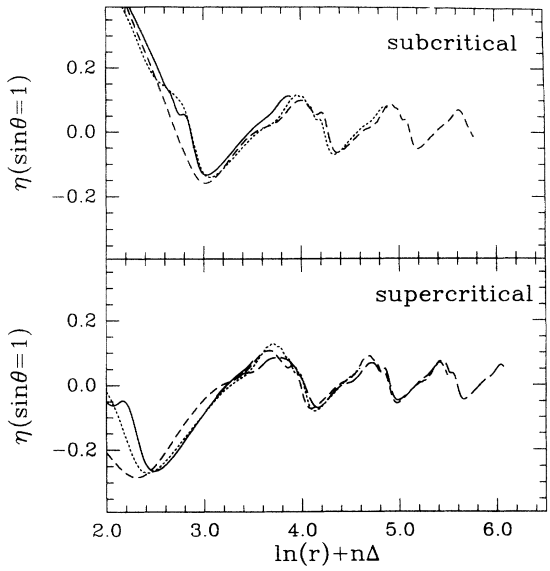

FIG. 6. Comparison of radial scaling in supercritical and subcritical models. Radial profiles of the metric function η, restricted to the symmetry plane $\theta = \pi/2$, are plotted. The upper frame shows profiles from a subcritical solution obtained at three epoches corresponding to alternate minima of the oscillations in α_0. The lower frame shows four profiles from a supercritical solution, which were also obtained at times of alternate central lapse minima. The radial profiles are shifted by $\rho \to \rho + n\Delta_\rho$ with $\Delta_\rho = 0.58$ in the subcritical case and $\Delta_\rho = 0.50$ in the supercritical case.

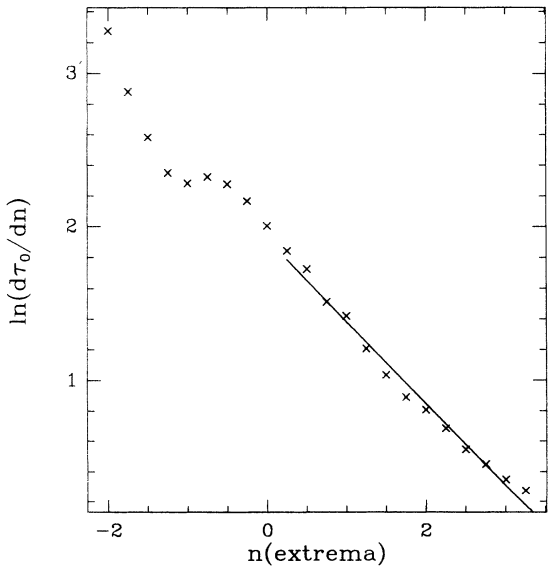

FIG. 5. Determination of the time-scaling constant Δ_τ for a near-critical evolution. The logarithm of the central proper time separation of corresponding central lapse extrema is plotted as a function of oscillation number. The critical oscillations are assumed to commence at $n = 0$. The quantity $d\tau/dn$ is computed and plotted for all of the four extrema comprising a single critical oscillation. The best fit to the slope gives $\Delta_\tau = 0.51$ and is indicated as the solid line.

ACKNOWLEDGMENTS

We thank Curt Cutler for an advance reading of the manuscript. This research was supported by NSF Grant Nos. PHY 90-07834 at Cornell University and PHY 90-01645 and PHY 90-57865 at the University of North Carolina. C.R.E. thanks the Alfred P. Sloan Foundation for research support. Computations were performed at the North Carolina Supercomputing Center and at the NSF supported Cornell Center for Theory and Simulation in Science and Engineering.

[1] M. W. Choptuik, Phys. Rev. Lett. **70,** 9 (1993).
[2] A. M. Abrahams and C. R. Evans, Phys. Rev. Lett. **70**, 2980 (1993) (paper 1).
[3] C. R. Evans and J. S. Coleman, Phys. Rev. Lett. (to be published).
[4] D. Christodoulou and S. Klainerman (unpublished).
[5] R. Beig and N. O'Murchadha, Phys. Rev. Lett. **66,** 2421 (1991).
[6] D. M. Eardley, in *Texas/PASCOS 92: Relativistic Astrophysics and Particle Cosmology*, Proceedings of the Workshop, Berkeley, California, 1992, edited by C. W. Akerlof and M. A. Srednicki [N.Y. Acad. Sci. **688**, 406 (1993)].
[7] S.-K. Ma, *Modern Theory of Critical Phenomena* (Addison-Wesley, Redwood City, 1976).
[8] J. W. York, in *Sources of Gravitational Radiation,* edited by L. Smarr (Cambridge University Press, Cambridge, 1979).
[9] A. M. Abrahams and C. R. Evans (unpublished).
[10] A. M. Abrahams and C. R. Evans, Phys. Rev. D **46**, R4117 (1992).
[11] See S. A. Teukolsky, Phys. Rev. D **26**, 745 (1982); C. R. Evans, in *Dynamical Spacetimes and Numerical Relativity*, edited by J. Centrella (Cambridge University Press, Cambridge, 1986); A. M. Abrahams and C. R. Evans, Phys. Rev. D **37**, 318 (1988).
[12] A. M. Abrahams and C. R. Evans, Phys. Rev. D **42**, 2585 (1990).